

SYNTHESIS, CHARACTERIZATION, CRYSTAL STRUCTURE, AND DFT STUDY OF 4-BROMO-2- (4,6-DICHLORO-PHENYLIMINO)-PHENOL

A. Soltani^{1,2*}, R. Mashkoor², A. D. Khalaji³,
S. G. Raz², S. H. Ghoran⁴, M. Dusek⁵,
K. Fejfarova⁵, and Y. Kanani²

The experimental crystal structure of a Schiff base compound 4-bromo-2-(4,6-dichloro-phenylimino)-phenol **1** is determined by single crystal X-ray diffraction and also characterized by FT-IR and ¹H NMR spectroscopy. The electronic structure in the gas phase is studied by density functional theory (DFT) calculations. The theoretical results have good agreement with the data obtained from the crystallographic analysis. In addition, theoretical configurations which refer to the title compound are relaxed and studied in terms of the combined analysis of HOMO-LUMO energy gap, total density of states (DOS), partial density of state (PDOS), overlap population density of state (OPDOS), molecular electrostatic potential (MEP), NMR spectra, and harmonic vibrational frequencies.

DOI: 10.1134/S0022476619060039

Keywords: Schiff base, single crystal, DFT calculation, electronic structure, NMR.

INTRODUCTION

Schiff bases ($-\text{CH}=\text{N}-$) are a class of structures which show different biological activities, including antitumor, antimicrobial, antifungal, and herbicidal properties. They are also applied for the preparation of a broad range of industrial compounds having a biological activity through reactions such as ring closure, cycloaddition, and replacement reactions. Other applications, e.g. the use as ligands in metal complexes, catalysis, dyes, and pigments, have also been reported [1-12]. In this work, the structure of 4-bromo-2-(4,6-dichloro-phenylimino)-phenol Schiff base was studied using ¹H NMR and FT-IR spectroscopic techniques. Its crystal structure was determined by single crystal X-ray diffraction. In addition, HOMO, LUMO, and NBO analysis were used to elucidate the information regarding charge transfer within the molecule. The optimized geometries, electronegativity (χ), electronic chemical potential (μ), global softness (S), global hardness (η), and electrophilicity index (ω) [13, 14] were calculated.

¹Golestan Rheumatology Research Center, Golestan University of Medical Sciences, Gorgan, Iran;
*Alireza.soltani46@yahoo.com. ²Young Researchers and Elite Club, Gorgan Branch, Islamic Azad University, Gorgan, Iran.
³Department of Chemistry, Faculty of Science, Golestan University, Gorgan, Iran. ⁴Young Researchers and Elite Club, Maragheh Branch, Islamic Azad University, Maragheh, Iran. ⁵Institute of Physics of the ASCR, v.v.i., Prague, Czech Republic. Original article submitted July 4, 2018; revised July 4, 2018; accepted September 11, 2018.

EXPERIMENTAL

Materials and methods. All reagents and solvents for the synthesis and spectroscopic studies were commercially available and used without further purification. The ^1H NMR spectra were measured by a BRUKER DRX-500 AVANCE spectrometer at 500 MHz, and all chemical shifts are reported in δ units downfield from TMS. The IR spectrum was recorded on a JASCO 680 plus FT-IR spectrophotometer as a KBr pellet.

Synthesis of 4-bromo-2-(2,5-dichloro-phenylimino)-phenol (1). The compounds of 5-bromo salicylaldehyde (0.168 g) and 2,4-dichloroaniline (0.201 g) were dissolved in methanol (10 mL) and then refluxed at 45 °C for 45 min to give a precipitate in a clear solution (Fig. 1). Then the precipitate was stirred, filtered off, and washed with methanol (5 mL). Suitable crystals for the X-ray diffraction analysis were formed by slow evaporation of the solvent after 24 h at room temperature.

Crystallographic data collection and refinement. A single crystal of the dimensions 0.47×0.07×0.03 mm was chosen for the X-ray diffraction study. Crystallographic measurements were made at 120 K with a four-circle Oxford Diffraction Gemini CCD diffractometer with mirror-collimated $\text{Cu}K_{\alpha}$ radiation ($\lambda = 1.5418 \text{ \AA}$) and an Atlas CCD detector. The crystal structures were solved by direct methods with the SIR2002 program [15] and refined with the Jana2006 program package [16] by the full-matrix least-squares technique on F^2 . The molecular structure plots were prepared by ORTEP III [17]. Hydrogen atoms were mostly discernible in different Fourier maps and could be refined to reasonable geometry. According to common practice, they were nevertheless kept in ideal positions during the refinement. The isotropic atomic displacement parameters of hydrogen atoms were evaluated at $1.2U_{\text{eq}}$ of the parent atom. We found that compound **1** crystallized in an orthorhombic crystal system, space group $P2_12_12_1$ with $a = 4.3701(2) \text{ \AA}$, $b = 12.9255(7) \text{ \AA}$, $c = 22.3779(13) \text{ \AA}$, and $V = 1264.03(12) \text{ \AA}^3$. Selected bond lengths and angles of **1** are listed in Table 1.

Computational methods. In this study, all computations were performed via the Gaussian 98 package [18] at the density functional theory (DFT) level using the hybrid B3LYP exchange functional. All molecular geometries are optimized using the standard 6-311++G** basis set at the B3LYP and HF levels [19-21]. Vibrational frequencies, natural bond orbital (NBO), and nuclear magnetic resonance (NMR) within GIAO were calculated with the B3LYP method and the 6-311++G** standard basis set [22-24]. Quantum molecular descriptors [22, 24] for this complex were determined as follows:

$$\chi = -\mu, \quad (1)$$

$$\eta = (I - A)/2, \quad (2)$$

where μ is the electronic chemical potential defined as the negative value of the electronegativity. In addition, the global softness S of the equilibrium state of an electronic system at a temperature T is defined as

$$S = 1/2\eta. \quad (3)$$

Recently, Parr and co-workers [25, 26] have introduced the electrophilicity index (ω) as

$$\omega = \mu^2/2\eta. \quad (4)$$

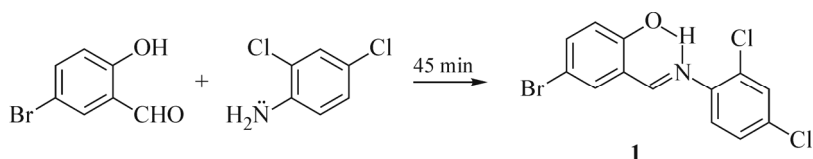


Fig. 1. Chemical structure of 4-bromo-2-(2,4-dichloro-phenylimino)-phenol **1**.

TABLE 1. Comparison of Selected Bond Lengths (Å) and Bond Angles (deg) for Compound **1** as Determined from the X-ray Structure Analysis and DFT Calculations

Parameter	Bond lengths			Parameter	Bond angles		
	Exp.	B3LYP	HF		Exp.	B3LYP	HF
Br1–C12	1.91(5)	1.91	1.90	C9–O1–H1	109.00(5)	109.11	110.68
Cl1–N1	2.91(4)	2.99	2.96(8)	Cl1–N1–C1	67.5(2)	66.01	65.43
O1–C9	1.34(6)	1.35	1.34	Cl1–N1–C7	168.8(3)	167.32	167.17
O1–H1	0.82(7)	0.97	0.95	C1–N1–C7	123.0(4)	119.38	119.05
N1–C1	1.41(7)	1.40	1.40	N1–C1–C2	117.9(4)	119.82	120.08
N1–C7	1.27(6)	1.28	1.25	N1–C1–C6	125.3(5)	122.72	122.11
C1–C2	1.40(7)	1.41	1.39	C2–C1–C6	116.8(5)	117.32	117.71
C1–C6	1.41(6)	1.41	1.39	C1–C2–C3	122.8(4)	121.65	121.36
C2–C3	1.39(7)	1.39	1.38	C2–C3–C4	117.6(4)	119.08	119.38
C3–C4	1.39(16)	1.38	1.37	C2–C3–H3	121.20	120.14	120.01
C4–C5	1.38(7)	1.39	1.38	C4–C3–H3	121.20	120.77	120.60
C5–C6	1.44(7)	1.39	1.38	C3–C4–C5	121.8(5)	121.05	120.74
C7–C8	1.43(6)	1.46	1.48	N1–C7–C8	121.8(4)	125.28	125.56
C8–C9	1.36(7)	1.42	1.40	N1–C7–H7	119.08	120.98	120.90
C8–C13	1.40(7)	1.41	1.39	Br1–C12–C11	119.6(4)	119.81	120.12
C9–C10	1.37(7)	1.40	1.39	Br1–C12–C13	119.6(4)	119.90	120.04
C10–C11	1.99(6)	1.39	1.38	C9–C10–C11	121.0(5)	121.34	121.20
C11–C12	1.99(6)	1.39	1.38	O1–C9–C8	121.6(5)	121.45	121.06
C12–C13	1.99(6)	1.39	1.38	O1–C9–C10	119.1(4)	119.04	119.45

It was proposed as a measurement of the electrophilic power of a molecule. The electronic chemical potential (μ) can be approximated as

$$\mu = -(I + A)/2, \quad (5)$$

where I ($-E_{\text{HOMO}}$) is the ionization potential and A ($-E_{\text{LUMO}}$) is the electron affinity of the molecule. E_{HOMO} are the energies of the highest occupied molecular orbital, plus the first given value of the valence band, E_{LUMO} are the energies of the lowest unoccupied molecular orbital. Thus, hard molecules have a large HOMO–LUMO gap and soft molecules have a small one. The frontier molecular orbitals (FMO) play an important role in the electrical and optical properties, as well as in UV-Vis spectra and chemical reactions. The operational definition of the hardness (η) was obtained using a finite difference approximation to the second derivative in Eq. (2), where I and A are the ionization potential and the electron affinity of the system, respectively.

High μ values and low η values characterize it as a good electrophile species. The maximum electronic charge ΔN_{max} of the electrophile system is given by Eq. (6) as

$$\Delta N_{\text{max}} = -\mu/\eta. \quad (6)$$

RESULTS AND DISCUSSION

^1H NMR spectra. First of all, we report the theoretical and experimental values for the ^1H NMR spectrum of compound **1**. The ^1H NMR spectrum of **1** was recorded using CDCl_3 . The O–H and N–H protons are observed as singlets at 12.97 ppm and 8.54 ppm, respectively. The aromatic protons are observed between 6.94–7.52 ppm. The ^1H NMR chemical shifts of **1** were computed within the GIAO approach at the B3LYP/6-311++G** level. The signals in the range 5.79–7.68 ppm are assigned to $\text{H}_2\text{–H}_8$ atoms, which is in good agreement with the experimental value. Our results demonstrate that the total numbers of protons are in agreement with the experimental values.

FT-IR spectra. In the FT-IR spectrum of **1**, vibration bands with the wavenumbers of 3430 cm^{-1} ($\nu\text{ O-H}$), 3079 cm^{-1} ($\nu\text{ C-H aromatic}$), 2626 cm^{-1} ($\nu\text{ H-C=N-}$), 1618 cm^{-1} ($\nu\text{ C=N}$), and 1468 cm^{-1} , 1579 cm^{-1} ($\nu\text{ C=C aromatic}$) were observed. The harmonic vibrational frequencies of **1** were calculated at the B3LYP/6-311++G** level. The predicated bonds at 3175 cm^{-1} , 3204 cm^{-1} , 3210 cm^{-1} , 3227 cm^{-1} , 3228 cm^{-1} , and 3240 cm^{-1} are assigned to aromatic ring C-H stretching vibrations. The C=C stretching vibrations in aromatic rings are observed at 1460 cm^{-1} , 1540 cm^{-1} , and 1599 cm^{-1} . In the calculated spectrum, for C=N a very strong bond is revealed at 1624 cm^{-1} and for O-H stretching vibrations a wide bond is observed at 3490 cm^{-1} at the B3LYP/6-311++G** level. In the theoretical spectrum, the bond observed at 1118 cm^{-1} is attributed to the C-Br stretching and benzene ring C-H rocking vibrations [27], while in the experimental spectrum the C-Br bond is observed at 811 cm^{-1} [28]. The C-Cl vibration is experimentally observed at 790 cm^{-1} and theoretically calculated by DFT/B3LYP at 769 cm^{-1} . Sudha et al. reported that the C-Cl stretching bond was observed at 919 cm^{-1} [29]. The theoretical and experimental calculations performed are very close to each other.

Crystal structure. An ORTEP view of **1**, including the atom-numbering scheme, is presented in Fig. 2. The N(1)-C(7) bond length is in agreement with the double bond for the imine group, while the N(1)-C(1) bond length is in agreement with single bonds of the amine groups. The molecule is almost planar, with a maximum deviation of $0.112(1)\text{ \AA}$ for Br1 from the least-squares plane through all the non-H atoms. The molecular conformation of **1** obtained from HF and DFT calculations shows a good agreement with the X-ray results (Table 1). The computed structural parameters of **1** are listed in Table 1. The slight differences between the computational and experimental parameters can be attributed to the fact that the HF and DFT methods were carried out with isolated molecules in the gas phase whereas the X-ray parameters were based on molecules in the solid state.

The computed total energies, dipole moment, and relative stability of 4-bromo-2-(4,6-dichloro-phenylimino)-phenol were studied. The relaxed bond lengths and angles of **1** calculated using Becke 3–Lee–Yang–Parr (B3LYP) and HF methods and the standard 6-311++G** basis set are calculated. The atom numbering scheme for the title molecule is given in Fig. 2. The average N1-C1 distance is about 1.40 \AA and 1.40 \AA computed via B3LYP and HF methods, respectively, while the N1-C1 distance for the experimental data is approximately 1.41 \AA . The N1-C7 distance is 1.28 \AA and 1.25 \AA from the B3LYP and HF methods, respectively. For the experimental result, the N1-C7 bond length is almost 1.27 \AA . Therefore, our computations indicate a slight deviation when they are compared with the experimental results. The calculated bond angle N1-C7-H7 = 119.08° (X-ray data) while this angle is 120.98° and 120.90° , according to the B3LYP and HF calculations respectively. The C4-C5-Br12 bond angle found by Karabacak et al. in 2-amino-5-bromobenzoic acid is 119.0° [30]. As can be observed in Table 1, the Br1-C12-C13 bond angle is 119.6° (experimental data), indicating excellent agreement with the theoretical data.

HOMO-LUMO analysis. The HOMO and LUMO are the main orbitals taking part in chemical stability [31]. The HOMO represents the ability to donate the electron, and the LUMO acts as an electron acceptor. The HOMO and LUMO energies were computed at the B3LYP and HF levels. Electronic transition absorption corresponds to the transition from the ground to the first excited state and is mainly described by electron excitation from HOMO to LUMO. The HOMO is

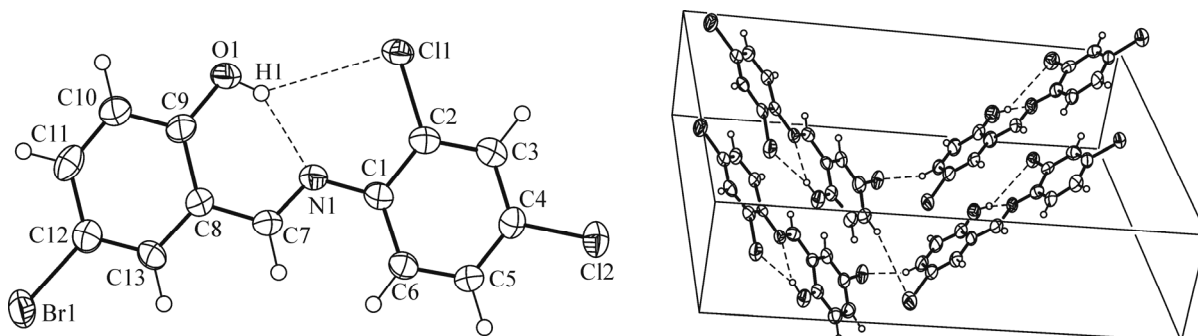


Fig. 2. Displacement ellipsoids of **1** with atomic numbering and the packing of the four molecules of **1** in the unit cell.

localized over the oxygen, bromine, and chlorine atoms, while the LUMO is localized over the C–C and C–N bonds and slightly on oxygen and chlorine atoms (Fig. 3). Both B3LYP and HF methods are applied to consider the HOMO and LUMO of the BDP compound. The notable difference occurred in E_{HOMO} obtained by the HF method (-8.45 eV) in comparison with E_{LUMO} that is approximately equal to each other with a value of 1.59 eV. DOS, PDOS, and OPDOS of this structure were calculated. The electronic structure of this compound is calculated by the DOS spectrum. OPDOS is the most important application of the DOS spectrum, indicating MO compositions and their contributions to the chemical bonding. OPDOS indicates the bonding, antibonding, and nonbonding properties of the reaction of the two orbitals, atoms, or groups. Also,

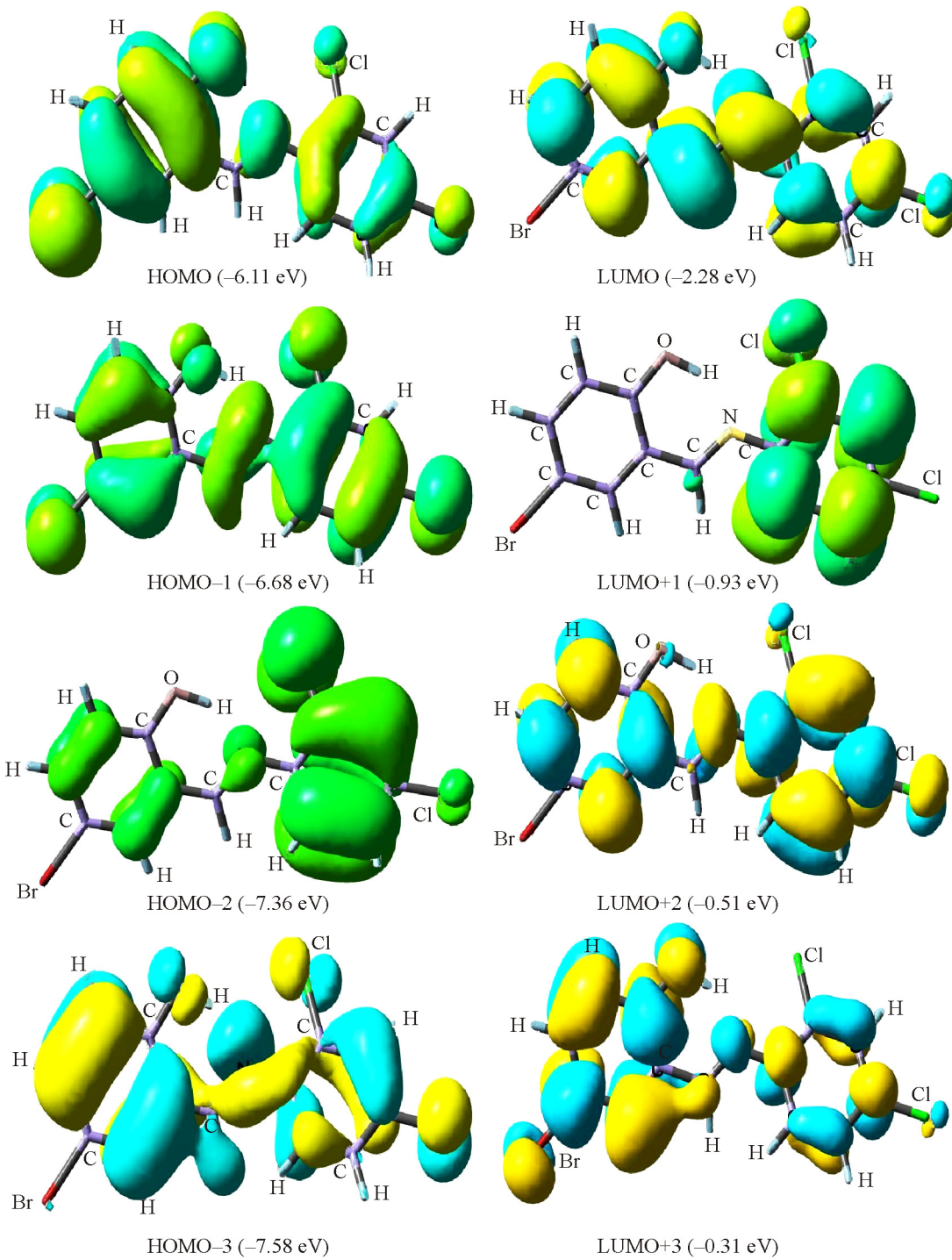


Fig. 3. HOMO and LUMO of compound **1**.

OPDOS represents a bonding interaction with a positive value (owing to the positive overlap population), the zero value shows nonbonding interactions, and a negative value corresponds to an antibonding interaction (owing to the negative overlap population).

The energy gaps are 3.83 eV (B3LYP) and 10.35 eV (HF) at both levels, which is an important stability for the molecule [32-34]. The μ_D value of this compound is reported of about 1.77 D (B3LYP) and 2.04 D (HF). The total energy is quite different for the two applied basis sets: -4122.27 a.u. (B3LYP) and -4115.10 a.u. (HF). The data of NBO and Mulliken charge analyzes for the **1** molecule were calculated. As shown in Table 2, the Mulliken population charges (MPA) for O and N atoms of the **1** molecule are about -0.642 a.u. and -0.580 a.u. (B3LYP) and -0.633 a.u. and -0.542 a.u. (HF). The NBO charge for O and N atoms of the **1** molecule are about -0.678 a.u. and -0.510 a.u. (B3LYP) and about -0.671 a.u. and -0.497 a.u. (HF). Moreover, the charge distribution can be explicated by molecular electrostatic potential (MEP) calculations. The hydrogen atoms of the molecule are relatively positive charged, as indicated by blue colors and a low intensity, while the oxygen atom of the molecule is negatively charged, as shown by the red color and a high intensity [35]. The chlorine and bromine atoms with the light green color upon them reveal that the point charge of the atoms is relatively zero.

Quantum molecular descriptors. Resistance towards deformation in the presence of an electric field is defined as the global hardness. The global hardness decreases with growing reactivity and increases with growing stability of the compound. The global hardness (η) of 1.92 eV calculated at the B3LYP level for the **1** molecule is significantly decreased as compared to the value of 5.04 eV obtained by the HF method. The chemical potential (μ) of -4.19 eV calculated at the

TABLE 2. Comparison of Selected Natural Charges for Compound **1**

Property	B3LYP		HF	
	MPA	NBO	MPA	NBO
C1–C2	0.304/-0.105	0.121/-0.032	0.280/-0.097	0.118/-0.038
C2–C3	-0.105/-0.146	-0.032/-0.255	-0.097/-0.150	-0.038/-0.251
C3–C4	-0.146/-0.058	-0.255/-0.041	-0.150/-0.054	-0.251/-0.046
C4–C5	-0.058/-0.142	-0.041/-0.242	-0.054/-0.143	-0.046/-0.240
C5–C6	-0.142/-0.149	-0.242/-0.231	-0.143/-0.143	-0.240/-0.231
C6–C7	-0.149/0.304	-0.231/0.121	-0.143/0.280	-0.231/0.118
C7–C8	0.107/0.079	0.135/-0.189	0.102/0.094	0.141/-0.184
C8–C9	0.079/0.322	-0.189/0.389	0.094/0.307	-0.184/0.381
C9–C10	0.322/-0.162	0.389/-0.275	0.307/-0.157	0.381/-0.270
C10–C11	-0.162/-0.144	-0.275/-0.206	-0.157/-0.146	-0.270/-0.207
C11–C12	-0.144/0.075	-0.206/-0.144	-0.146/0.084	-0.207/-0.146
C12–C13	0.075/-0.222	-0.144/-0.200	-0.084/-0.230	-0.146/-0.201
C13–C8	-0.222/0.079	-0.200/-0.189	-0.230/0.094	-0.201/-0.184
C2–Cl1	-0.105/0.017	-0.032/0.023	-0.097/0.016	-0.038/0.026
C4–Cl2	-0.058/-0.004	-0.041/0.011	-0.054/-0.003	-0.046/0.015
C9–O1	0.322/-0.642	0.389/-0.678	0.307/-0.633	0.381/-0.671
C7–N1	0.107/-0.580	0.135/-0.510	0.102/-0.542	0.141/-0.497
C12–Br1	0.075/-0.130	-0.144/0.056	0.084/-0.133	-0.146/0.060
C7–H1	0.107/0.148	0.135/0.202	0.102/0.142	0.141/0.194
C13–H2	-0.222/0.157	-0.200/0.252	-0.230/0.154	-0.201/0.249
O1–H3	-0.642/0.455	-0.678/0.521	-0.633/0.445	-0.671/0.517

B3LYP level is slightly larger than -3.45 eV obtained by the HF method. The electrophilicity index is a measurement of the electrophilic power of a molecule. It determines the ligand energy lowering and contains information on the structural stability, reactivity, and toxicity of chemical species [35]. The electrophilicity index found for **1** was 4.57 eV at the B3LYP level and 1.18 eV found by the HF method. Our computational results reveal that the molecular reactivity is different in both methods.

CONCLUSIONS

In summary, compound **1** was synthesized and its crystal and molecular structures were determined. The compound was characterized by FT-IR and ^1H NMR spectroscopy. The DFT-predicted relaxed geometry and vibrational spectra were analyzed through comparing with the experimental values and indicate good agreement. The bond lengths and bond angles of the compound calculated by the B3LYP method in the gas phase were in a good agreement with the reported X-ray crystal data. The electronic properties and geometric parameters were analyzed at the B3LYP and HF levels of theory.

ACKNOWLEDGMENTS

We thank the Sayad Shirazi Hospital, Golestan University of Medical Sciences, Gorgan, Iran. We also thank the Islamic Azad University (Gorgan Branch) as well as the Golestan University (GU) for partial support of this work.

FUNDING

Crystallographic part was supported by project 14-03276S of the Grant Agency of the Czech Republic.

ADDITIONAL INFORMATION

Crystallographic data (excluding structure factors) for the structure reported in this paper have been deposited with the Cambridge Crystallographic Center. Copies of the data can be obtained free of charge on application to The Director, CCDC, 12 Union Road, Cambridge CB2 1EZ, UK, fax: +44 1223 336 033, e-mail: deposit@ccdc.cam.ac.uk or <http://www.ccdc.cam.ac.uk>.

CONFLICT OF INTERESTS

The authors declare that they have no conflict of interests.

REFERENCES

1. A. Dehno Khalaji, A. Najafi Chermahini, K. Fejfarova, and M. Dusek. *Struct. Chem.*, **2010**, *21*, 153–157.
2. A. Dehno Khalaji, M. Weil, G. Grivani, and S. Jalali Akerdi. *Monatsh Chem.*, **2010**, *141*, 539–543.
3. M. Morshedi, M. Amirmasr, S. Triki, and A. Dehno Khalaji. *J. Chem. Crystallogr.*, **2011**, *41*, 39–43.
4. A. Dehno Khalaji and H. Stoekli-Evans. *Polyhedron*, **2009**, *28*, 3769–3773.
5. A. Dehno Khalaji, M. Weil, H. Hadadzadeh, and M. Daryanavard. *Inorg. Chim. Acta*, **2009**, *362*, 4837–4842.
6. A. Dehno Khalaji, H. Hadadzadeh, K. Fejfarova, and M. Dusek. *Polyhedron*, **2010**, *29*, 807–812.
7. B. Kumar Paul and N. Guchhait. *Chem. Phys.*, **2013**, *412*, 58–67.
8. G. Bator, L. Sobczyk, W. Sawka-Dobrowolska, J. Wuttke, A. Pawlukojc, E. Grech, and J. Nowicka-Scheibe. *Chem. Phys.*, **2013**, *410*, 55–65.
9. M. Małecka, S. Mebs, and A. Jozwiak. *Chem. Phys.*, **2012**, *407*, 20–28.
10. E. Fereyduni, M. K. Rofouei, M. Kamaee, S. Ramalingam, and S. M. Sharifkhani. *Spectrochim. Acta A*, **2012**, *90*, 193–201.

11. A. Dehno Khalaji, S. Mehrani, V. Eigner, and M. Dusek. *J. Mol. Struct.*, **2013**, *1047*, 87–94.
12. A. Dehno Khalaji, M. Nikookar, K. Fejfarova, and M. Dusek. *J. Mol. Struct.*, **2014**, *1071*, 6–10.
13. A. Soltani, S. Ghafouri Raz, M. Ramezani Taghartapeh, A. Varasteh Moradi, and R. Zafar Mehrabian. *Comput. Mater. Sci.*, **2013**, *79*, 795–803.
14. M. Kia, M. Golzar, K. Mahjoub, and A. Soltani. *Superlattic. Microstruct.*, **2013**, *62*, 251–259.
15. M. C. Burla, M. Camalli, B. Carrozzini, G. Casciaro, C. Giacovazzo, G. Polidori, and R. Spagna. *J. Appl. Cryst.*, **2013**, *36*, 1103.
16. V. Petricek, M. Dusek, and L. Palatinus. Jana2006. Structure Determination Software Programs. Institute of Physics, Praha, Czech Republic, **2008**.
17. L. J. Farrugia. *J. Appl. Cryst.*, **1997**, *30*, 656.
18. M. J. Frisch, G. W. Trucks, H. B. Schlegel, G. E. Scuseria, M. A. Robb, J. R. Cheese-man, V. G. Zakrzewski, J. A. Montgomery Jr., R. E. Stratmann, J. C. Burant, S. Dapprich, J. M. Millam, A. D. Daniels, K. N. Kudin, M. C. Strain, O. Farkas, J. Tomasi, V. Barone, M. Cossi, R. Cammi, B. Mennucci, C. Pomelli, C. Adamo, S. Clifford, J. Ochterski, G. A. Petersson, P. Y. Ayala, Q. Cui, K. Morokuma, D. K. Malick, A. D. Rabuck, K. Raghavachari, J. B. Foresman, J. Cioslowski, J. V. Ortiz, A. G. Baboul, B. B. Stefanov, G. Liu, A. Liashenko, P. Piskorz, I. Komaromi, R. Gomperts, R. L. Martin, D. J. Fox, T. Keith, M. A. Al-Laham, C. Y. Peng, A. Nanayakkara, C. Gonzalez, M. Challacombe, P. M. W. Gill, B. Johnson, W. Chen, M. W. Wong, J. L. Andres, C. Gonzalez, M. Head-Gordon, E. S. Replogle, and J. A. Pople. Gaussian 98, Gaussian Inc., Pittsburgh, PA, **1998**.
19. A. Soltani, A. Varasteh Moradi, M. Bahari, A. Masoodi, and S. Shojaee. *Physica B*, **2013**, *430*, 20–26.
20. I. Novak and B. Kovac. *Chem. Phys. Lett.*, **2011**, *510*, 57–59.
21. J. M. Oliva and A. Vegas. *Chem. Phys. Lett.*, **2012**, *533*, 50–55.
22. A. Soltani, M. T. Baei, E. Tazikeh Lemeski, and M. Shahini. *Superlattic. Microstruct.*, **2014**, *76*, 315–325.
23. N. Saikia and R. C. Deka. *Computat. Theo. Chem.*, **2011**, *964*, 257–261.
24. T. Koopmans. *Physica*, **1933**, *1*, 104.
25. R. G. Parr and W. Yang. Density Functional Theory of Atoms and Molecules. Oxford University Press: New York, **1989**.
26. R. G. Parr and R. G. Pearson. *J. Am. Chem. Soc.*, **1983**, *105*, 7512.
27. N. Gunaya, E. Tarcan, D. Avcıb, K. Esmera, and Y. Atalay. *Z. Naturforsch.*, **2009**, *64a*, 745–752.
28. A. Dehno Khalaji and F. Malekan. *J. Clust. Sci.*, **2014**, *25*, 517–521.
29. S. Sudha, N. Sundaraganesan, M. Kurt, M. Cinar, and M. Karabacak. *J. Mol. Struct.*, **2011**, *985*, 148–156.
30. M. Karabacak and M. Cinar. *Spectrochim. Acta Part A*, **2012**, *86*, 590–599.
31. S. Subashchandrabose, A. R. Krishnan, H. Saleem, V. Thanikachalam, G. Manikandan, and Y. Erdogan. *J. Mol. Struct.*, **2010**, *981*, 59–70.
32. D. F. V. Lewis, C. Ioannides, and D. V. Parke. *Xenobiotica*, **1994**, *24*, 401.
33. S. Sebastian, S. Sylvestre, N. Sundaraganesan, M. Amalanathan, S. Ayyapan, K. Odayakumar, and B. Karthikeyan. *Spectrochim. Acta A*, **2013**, *107*, 167–178.
34. M. Karabacak and M. Cinar. *Spectrochim. Acta Part A*, **2012**, *86*, 590–599.
35. A. Soltani, F. Ghari, A. Dehno Khalaji, E. Tazikeh Lemeski, K. Fejfarova, M. Dusek, and M. Shikhi. *Spectrochim. Acta A*, **2015**, *139*, 271–278.